

Earth's Future

RESEARCH ARTICLE

10.1029/2023EF004334

Key Points:

- 2/3 of the interannual variations in area burned are explained by climate in a substantial portion of the world's burnable regions
- Same-fire-season weather is moderately more important than antecedent-fire-season weather for burned area variability
- Burned area is associated with antecedent wet and cool periods especially in the more arid areas

Supporting Information:

Supporting Information may be found in the online version of this article.

Correspondence to:













A. Gincheva,
andrina@um.es

Citation:

Gincheva, A., Pausas, J. G., Torres-Vázquez, M. Á., Bedia, J., Vicente-Serrano, S. M., Abatzoglou, J. T., et al. (2024). The interannual variability of global burned area is mostly explained by climatic drivers. *Earth's Future*, 12, e2023EF004334. <https://doi.org/10.1029/2023EF004334>

Received 21 DEC 2023
Accepted 8 MAY 2024

The Interannual Variability of Global Burned Area Is Mostly Explained by Climatic Drivers

Andrina Gincheva¹ , Juli G. Pausas² , Miguel Ángel Torres-Vázquez¹ , Joaquín Bedia³ , Sergio M. Vicente-Serrano⁴ , John T. Abatzoglou⁵ , Josep A. Sánchez-Espigares⁶ , Emilio Chuvieco⁷ , Sonia Jerez¹ , Antonello Provenzale⁸ , Ricardo M. Trigo⁹ , and Marco Turco¹ 

¹Department of Physics, Regional Atmospheric Modelling Group, Regional Campus of International Excellence Campus Mare Nostrum, University of Murcia, Murcia, Spain, ²Centro de Investigaciones sobre Desertificación (CIDE, CSIC-UV-GVA), Spanish National Research Council, Valencia, Spain, ³Departamento de Matemática Aplicada y Ciencias de la Computación, Grupo de Meteorología y Computación, Universidad de Cantabria, Unidad Asociada al CSIC, Santander, Spain, ⁴Instituto Pirenaico de Ecología (IPE-CSIC), Consejo Superior de Investigaciones Científicas, Zaragoza, Spain, ⁵Management of Complex Systems, University of California, Merced, CA, USA, ⁶Department of Statistics and Operations Research, Polytechnic University of Catalonia, Barcelona, Spain, ⁷Department of Geology, Geography and the Environment, Universidad de Alcalá, Environmental Remote Sensing Research Group, Alcalá de Henares, Spain, ⁸Institute of Geosciences and Earth Resources, National Research Council, Pisa, Italy, ⁹Faculdade de Ciências, Instituto Dom Luiz (IDL), Universidade de Lisboa, Lisboa, Portugal

Abstract Better understanding how fires respond to climate variability is an issue of current interest in light of ongoing climate change. However, evaluating the global-scale temporal variability of fires in response to climate presents a challenge due to the intricate processes at play and the limitation of fire data. Here, we investigate the links between year-to-year variability of burned area (BA) and climate using BA data, the Fire Weather Index (FWI), and the Standardized Precipitation Evapotranspiration Index (SPEI) from 2001 to 2021 at ecoregion scales. Our results reveal complex spatial patterns in the dependence of BA variability on antecedent and concurrent weather conditions, highlighting where BA is mostly influenced by either FWI or SPEI and where the combined effect of both indicators must be considered. Our findings indicate that same-season weather conditions have a more pronounced relationship with BA across various ecoregions, particularly in climatologically wetter areas. Additionally, we note that BA is also significantly associated with periods of antecedent wetness and coolness, with this association being especially evident in more arid ecoregions. About 60% of the interannual variations in BA can be explained by climatic variability in a large fraction (~77%) of the world's burnable regions.

Plain Language Summary In the context of changing climatic conditions, it is increasingly important to better understand the relationship between climate and fires. This study proposes a method that evaluates climatic conditions, either antecedent to or coincident with the fire season or the composite effect of both. It shows that the interannual variability of the global burned area for the period 2001 to 2021 is explained by climatic factors by around 60%. Our results also indicate that climatic drivers concurrent to the fire season prevail moderately over the antecedents. This suggests that the expected increase in burned area due to warmer and/or drier conditions can be mitigated where these climate conditions limit fuel availability.

1. Introduction

Fire plays a crucial role in the Earth's System, with widespread impacts on the carbon cycle, ecosystems, and both humans and wildlife. It is estimated that, on average, more than 4 million km² burn every year at a global scale (Bowman et al., 2020), but this is an underestimation, as the smallest fires are not considered (Chuvieco et al., 2019; Ramo et al., 2021). In areas with a dense urban-wildland interface, wildfires often have devastating consequences (Coughlan et al., 2019). Overall, there is a rising concern over potential changes in wildfire patterns related to climate change, and there is strong evidence that the weather conditions triggering and sustaining wildfires will become more frequent at higher levels of global warming (IPCC, 2021).

Understanding how fires respond to climate variability is crucial in light of ongoing climate change. However, despite the availability of newly accessible data sets and increasing research efforts that have advanced our

understanding of this topic, many aspects of this relationship remain unclear (Jones et al., 2022). Specifically, determining the temporal links between climate and fire is a major challenge due to the limited availability of comprehensive fire data sets on a global scale (Bowman, 2018; Bowman et al., 2020) and the complex interplay of multiple drivers (Pausas & Keeley, 2021).

Numerous studies have explored the spatial links of global scale effects of climatology on fire statistics averaged over a specific period of time (see e.g., Chuvieco et al., 2021; Krawchuk & Moritz, 2011). However, understanding how temporal variations in climate drive fire fluctuations at a global scale has received less attention, primarily because there is a dearth of comprehensive long-term global fire data necessary to determine reliable statistical links (Abatzoglou & Williams, 2016; Le Page et al., 2008). A better understanding of the dynamic links concerning climate and fire may support the development of predictive models (Chen et al., 2016; Shen et al., 2019; Turco, Jerez, et al., 2018).

On the other hand, at a regional scale, the temporal link between fires and climate was generally analyzed in data-rich areas. Such analyses demonstrated that climate is a significant driver of the interannual variability in BA, in many cases being the primary factor in explaining BA variability (Urbietta et al., 2015; Vadrevu et al., 2019; Zubkova et al., 2019; see also Jones et al., 2022, and references therein). For instance, in western US forests, 76% of the year-to-year variability in BA is explained by climate indices (Abatzoglou & Williams, 2016). Similarly, between 60% and 80% of the interannual BA variability can be explained by climate variables in Canadian ecoregions (Balshi et al., 2009; Girardin & Wotton, 2009). Strong links between BA and climate variations were also detected in southern Europe (Bedia et al., 2014; Turco et al., 2017; Turco, Jerez, et al., 2019) where fire danger and/or drought indices alone explained over 60% of the variability in BA. Likewise, forest BA in Australia is strongly linked to some climate indices, which explain more than two-thirds of the BA variance (Canadell et al., 2021). However, although relevant at a regional scale, these results provide limited insight into global patterns. In contrast to such regional studies, the pioneering work of Abatzoglou et al. (2018) indicates that climate variability explains only about one-third of the global interannual variability of BA. This comparatively smaller explained variance might be attributed to challenges stemming from the relatively short span of global fire observations available from satellites and potential inconsistencies in certain data sets as acknowledged by Abatzoglou et al. (2018). Additionally, Abatzoglou et al. (2018) opted for a relatively straightforward modeling approach, emphasizing simplicity and clarity. They limited their focus to a select set of well-established predictors, even though they recognized the potential benefits of a more elaborate model with expanded predictors.

Previous global studies (see e.g., Abatzoglou et al., 2018; Bedia et al., 2015; Grillakis et al., 2022) have indicated that the FWI is a good proxy for the climatic variables that influence fuel moisture and fire spread once ignited, and thus the burned area itself, at least in some regions. Precipitation is often used as an antecedent climate predictor (e.g., Xystrakis et al., 2014). On a global scale, Abatzoglou et al. (2018) used precipitation as the only climate variable to account for antecedent effects. On the other hand, the Standardised Precipitation Evapotranspiration Index (SPEI) is also a viable candidate both as a concurrent and an antecedent climate driver for BA variability (see e.g., Turco, Rosa-Cánovas, et al., 2018; Urbietta et al., 2015). Here we consider SPEI as an antecedent variable, as several analyses have shown that SPEI has higher predictive power than precipitation anomalies for hydrological, agricultural, and ecological impacts (e.g., Vicente-Serrano et al., 2012), including fires (Marcos et al., 2015; Turco, Rosa-Cánovas, et al., 2018). Thus, we evaluate SPEI as a potential predictor candidate for antecedent weather effects and SPEI and FWI as candidates for concurrent drivers. To sum up, here we model interannual BA variability by means of five models selected for each ecoregion, using the following predictor sets: (a) concurrent standardized FWI (SFWIc), (b) concurrent SPEI (SPEIc), (c) antecedent SPEI (SPEIa), (d) SFWIc and SPEIa, and (e) SPEIc and SPEIa. Our study thus extends previous studies (see e.g., Abatzoglou et al., 2018; Bedia et al., 2015; Turco, Jerez, et al., 2018) by incorporating a different combination of climate predictor variables explore the spatial patterns of the relationship between interannual fluctuations of BA and climate variability, at ecoregion scale over the entire globe.

2. Data and Methods

2.1. Data

Monthly BA data for the period 2001–2021 are obtained from the MODIS C6 data set (Giglio et al., 2018) that offers global BA coverage from November 2000 to September 2022 at a spatial resolution of 0.25°. This MCD64CMQ collection is derived from the MODIS C6 Terra and Aqua 500 m daily surface reflectance data sets

(namely MOD09GHK and MYD09GHK), combined with the 1 km daily level 3 MODIS active fire data sets (MOD14A1 and MYD14A1). A relatively recent comparative study between remote sensing data and official fire records in the Mediterranean region of Europe revealed that the MODIS C6 data set broadly matches other BA data (Turco, Herrera, et al., 2019). The analysis by Turco, Herrera, et al. (2019) evidences a strong temporal correlation ($\sim 0.5/0.6$) between BA data obtained from satellite data sets, including MODIS C6, and official national BA data. Additionally, we contrasted our results also considering the Fire_cci v5.1 data set (FireCCI51, Lizundia-Loiola et al., 2020), available for the period 2001–2020. For this data set, we consider two series of data, the original total BA, and the data filtering out the values from the land categories “cropland, rainfed,” “cropland, irrigated or post-flooding” and “mosaic cropland (>50%)” to evaluate if agricultural fires can alter the climate-fire links.

We analyzed two climate indices: the Standardized Precipitation Evapotranspiration Index (SPEI) (Vicente-Serrano et al., 2010) and the Fire Weather Index (FWI; Vitolo et al., 2020). The SPEI index is calculated by converting the difference between cumulative precipitation (PREC) and potential evapotranspiration (PET) over a specified period (in this case, 3, 6, and 12 months) into a Gaussian distribution. Positive values denote wet conditions, whereas negative values imply dry conditions compared to long-term climatology. We opted for the Multi-Source Weighted-Ensemble Precipitation (MSWEP version 2.8; Beck, Wood, et al., 2019) data set as our primary source for PREC data. We estimated the PET utilizing the FAO-56 Penman-Monteith equation based on daily data provided by the ERA5 global reanalysis (Hersbach et al., 2020). More details on the PET estimations are provided in Vicente-Serrano et al. (2022). We obtained the FWI version 4 data from the Copernicus Emergency Management Service (Vitolo et al., 2020), which is derived using meteorological data from the ERA5 reanalysis. We calculated the Standardized Fire Weather Index (SFWI) by standardizing the average monthly FWI values over 3, 6, or 12 months. This involves calculating an anomaly by subtracting the long-term mean from the original time series and dividing the anomaly by the standard deviation.

We use ecoregions as our fundamental working units, as defined by Dinerstein et al. (2017). Within each ecoregion, we aggregate BA through summation and climate data via arithmetic mean.

2.2. Deriving the Empirical Models of Fire Response to Climate Variations

Figure 1 depicts the primary stages of constructing our empirical climate-fire models. First, for each ecoregion, the fire season is determined (with details provided later). For illustrative purposes, we highlight the “Sierra Nevada Forests” ecoregion (USA). Here, the fire season encompasses the months of July–September. By summing up the BA over these months, we generate a 21-year time series of BA values. These series are subsequently log-transformed, detrended, and standardized. In the bottom plot, this is showcased as the Burned Area Index (BAI; depicted in black). We then explore models that might connect Coincident Climate variables and/or Antecedent Climate factors to BA. Further specifics about this search are discussed later. The model showcased here considers the coincident 6-month aggregated SPEI for July and demonstrates a reasonable fit, with a variance explained of 54%, aligning with findings from more localized and detailed data, as shown in Turco et al. (2023).

The developed fire climate-fire model (Gincheva & Turco, 2023) is based on aggregated BA data during the “fire season,” which is expressed as “[...] the minimum number of consecutive months containing more than 80% of the burned area,” according to the definition proposed by Abatzoglou et al. (2018). Using this definition, we extract the fire season for each ecoregion of the globe as follows. First, we aggregated the monthly BA data at the annual scale. To avoid including artifacts from isolated fires, only ecoregions with annual BA >0 in at least 2 years were considered for inclusion in the subsequent analysis. Then, we computed the climatological means of monthly BA values and arranged them in descending order. Consequently, we defined the fire season as the smallest number of uninterrupted months required to accumulate 80% of the total annual mean BA. Finally, the BA data are aggregated over this fire season. In addition, to avoid spurious model results due to infrequent fire events, we filter out those ecoregions that contributed to less than 0.001% of the global BA (as in Abatzoglou et al., 2018) and where BA was present in at least half or more of the available period. That is, we selected only those ecoregions where BA >0 in at least 10 years, following the criteria of Chen et al. (2016) and Turco, Jerez, et al. (2018). The spatial distribution of the months corresponding to the fire season for each ecoregion can be seen in Figure S1 in Supporting Information S1.

The data aggregated over the fire season, are subjected to a logarithmic transformation to address their skewness. To ensure the transformation is suitable for all values, including zeros, we add a unit equivalent to 1 ha before

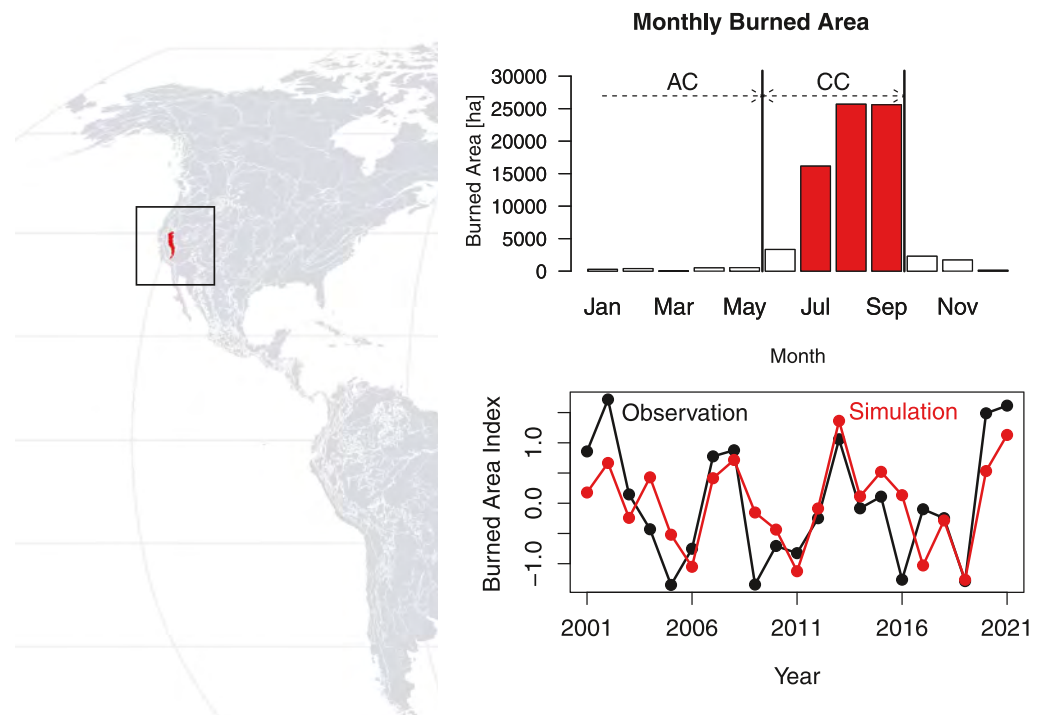


Figure 1. Schematic representation of the primary steps in deriving empirical climate-fire models. The red area in the upper left panel indicates the “Sierra Nevada Forests” ecoregion located in California, USA. The upper right panel shows the mean observed burned area for each month in that ecoregion, indicating with red bars the fire season. The terms “AC” and “CC” refer to Antecedent Climate and Coincident Climate, respectively. The lower right panel shows the time series of the Burned Area Index observed (in black) and simulated (in red).

applying the transformation (as in Parks & Abatzoglou, 2020). This adjustment makes the method applicable to the entire BA data set. To evaluate the sensitivity of our results to this transformation, we also considered the data transformed using a square root method. Unlike the logarithmic transformation, the square root transformation can be applied to BAI values that are zero, making it potentially more suitable for data sets that include these values. To assess the amount to which climate variability accounted for fluctuations in log-transformed BA, we first applied linear detrending to the all-time series, including both log-transformed BA and climate variables. This process is mathematically represented as:

$$\text{Detrended series} = \text{Original series} - (\beta_0 + \beta \times \text{Year}) \quad (1)$$

Where β_0 and β represent the intercept and slope, respectively, of the linear trend of the original series determined by the least squares method. This approach minimizes the influence of factors that change gradually over time, which is typically the case for changes in land use and fire management improvements. It thus isolates the effects of year-to-year variability in climate and BA. Additionally, to further explore the potential influence of nonlinear trends on the BA series, we repeat all the analyses considering a quadratic detrending method (Detrended series = Original series - ($\beta_0 + \beta_1 \times \text{Year} + \beta_2 \times \text{Year}^2$)). Moreover, all variables are standardized enabling the coefficients of climate predictors in the regression model to be comparable with each other.

Then, assuming that climate is the main driver of year-to-year variations in the log-transformed BA through two processes—control of fuel moisture and/or fine fuel biomass availability (indirectly through antecedent primary productivity)—we consider that concurrent climate variables (CC; i.e., within the same fire season) are effective proxies for controlling fuel moisture, while antecedent climate variables (AC) are suitable proxies for influencing fine fuel availability and structure. Thus, the possible dependence of BA on the climatic variables CC and AC is derived using the following equation:

$$BAI = a * AC_{ta,ma} + b * CC_{tb,mb} + \varepsilon \quad (2)$$

Where:

- BAI is the log-transformed, detrended and standardized time series of BA for the fire seasons for the period 2001–2021.
- Coefficients a and b represent the BAI sensitivity to detrended and standardized AC and CC, respectively.
- ta and tb are the accumulation periods (3, 6, or 12 months, as in Turco, Jerez, et al., 2018) used to calculate AC and CC, respectively.
- The months used to calculate AC and CC are denoted by ma and mb , respectively. Following Abatzoglou et al. (2018), we limit the search for mb to the 1-month buffer preceding the fire season and the final month of the fire season. In the example of Figure 1 with a fire season that includes the months July–August–September, the search would be conducted from June to September, and the best model for that ecoregion considers the SPEI for $tb = 6$ and $mb = 7$, that is, include the months from February through July.
- Again, following Abatzoglou et al. (2018), we restricted the search for ma to range from 14 to 2 months before the start of the fire season.
- Finally, ε is a term representing stochastic noise. In line with established protocols (refer to, e.g., Tong, 1990), we verified that the model's stochastic component adheres to a Gaussian distribution employing the Kolmogorov–Smirnov test (Massey, 1951), ensured that it is independent by using the Durbin–Watson statistic (Durbin & Watson, 1950), and assessed for non-heteroscedasticity with the Breusch–Pagan test (Breusch & Pagan, 1979).

2.3. Best Model Choice for Each Ecoregion

To choose the most suitable model for every ecoregion, we explore all potential temporal aggregations of the predictors through an out-of-sample calibration, while varying ma , ta , mb , and tb . Specifically:

- a) We evaluated all potential predictors by fitting all possible versions of Equation 1, together (i.e., the variables AC and CC) or individually (i.e., AC or CC), through a leave-one-year-out cross-calibration. Through iterative processing, we used each individual year in the original series set as test data while utilizing the remaining samples as data for training the model.
- b) Our main goal was to create an empirical model that considers the potential effect of climate on fires through the climate impacts on the quantity of dry biomass accessible for burning during a fire. For this, we assumed two simple restrictions. Namely, we only retained models whose coefficients of AC and CC conform to the hypothesis that CC regulates fuel flammability (e.g., we retain models with positive SFWI or negative SPEI coefficients) and AC represents antecedent climate that regulates anomalously high fine fuel production (e.g., we retain models with positive coefficients when SPEI is used as AC). This approach is similar to linear regression models with sign restriction, where signs are imposed on the coefficients of the regression model based on prior knowledge of the relationships between the explanatory variables and the response (see e.g., Kato et al., 2019; Silvapulle & Sen, 2005).
- c) We conduct a one-tailed hypothesis test to evaluate the significance of the individual (Pearson) correlations present within these models.
- d) We corrected the p -values of the individual correlation tests by means of the False Discovery Rate (FDR) technique (Ventura et al., 2004).
- e) Finally, we selected the model with the highest correlation value with an adjusted p -value < 0.05 .

Model selection using an out-of-sample procedure is equivalent to the use of the Akaike Information Criterion (Stone, 1977). Note that such a leave-one-out cross-calibration procedure allowed for the evaluation of out-of-sample BA records, as in an operational forecasting context (see e.g., Bedia et al., 2015). To avoid artificial skill in the cross-validation process, the observed climate series were detrended and standardized at each step. This ensured that observations from the predicted year were not used. Once the optimal climate windows were selected, we developed the final models using all available data (in-sample calibration). We selected, as final models, those whose coefficients were statistically significant (p -value < 0.05). For example, if after the out-of-sample selection, a model with the variables AC and CC was selected, but the in-sample model indicates that only the CC coefficient is statistically significant, the final model will only include the CC variable. We also

incorporated the Variance Inflation Factor (VIF) for the selection of our final models where both AC and CC were selected. Following the recommendation by Zuur et al. (2010), models with a VIF > 2 were flagged for potential multicollinearity issues. In such instances, we further evaluated the model with only CC to ensure robustness and reduce potential collinearity issues.

Finally, the link between time-invariant characteristics of the climate-fire models and the spatial climatology of PREC and PET (averaged over the period of the study 2001–2021) has been examined using generalized additive models (GAM), as implemented in the "mgcv" R package. GAMs facilitate the discovery of intricate relationships through smooth, non-parametric functions, offering a flexible approach to investigating non-linear dynamics. Such GAMs are commonly employed in bivariate analyses in similar studies to identify nonlinear associations (see e.g., Abatzoglou et al., 2018; Pausas, 2022).

3. Results

3.1. Variability of Burned Area Explained by Climate

Statistically significant links between climate and fire variability have been observed in roughly 77% of the study domain (or in 71% of the ecoregions analyzed), as shown in Figure 2a and in Table 1. On average, climate variability explains around 60% of the variance in BA over the past two decades, as presented in Table 1.

The best model varies across ecoregions (Figures 2b and 2c), with a similar fraction of multivariate models (i.e., those including both antecedent and concurrent climate drivers; 34%) and of monivariate models (37%). Concurrent variables (SPEIc or SFWIc) significantly contribute to explaining BA variability over 64% of the global burnable area, while antecedent SPEIa significantly contributes over 41% of the area (Table 1). Among the concurrent variables, the monivariate models with SFWIc contribute over 18% of the ecoregions, while the ones with SPEIc present over 12% of the ecoregions (Figure 2c).

The overarching conclusions of our study remain consistent across different methodological approaches (as summarized in Table S1 in Supporting Information S1). However, upon closer examination of Figures S2–S5 in Supporting Information S1, it is important to note that localized discrepancies are evident. These include variations in the best model outcomes for certain ecoregions (e.g., over parts of Eurasia, West Africa, and China) when comparing square root (Figure S2 in Supporting Information S1) and logarithmic transformations of BA, applying quadratic (Figure S3 in Supporting Information S1) versus linear detrending, or analyzing data from alternative satellite products (Figure S4 in Supporting Information S1) and with or without the inclusion of agricultural fires (Figure S5 in Supporting Information S1). Such differences, though not undermining our main findings, highlight the complexity of the climate-BA relationship and underscore the importance of considering multiple analytical perspectives.

3.2. Burned Area and Concurrent Weather

We assessed the sensitivity of BA to the concurrent predictor variables, SFWIc and SPEIc, using the coefficients of statistical regression models correlating climate with BA (see Figure 3a). Since these predictor variables are standardised with a mean of zero and a unit standard deviation, the sensitivity of the BA model gives us an indication of how BAI adjusts with a unit change in these concurrent factors. The analysis reveals that the sensitivity of BAI to SFWIc is 0.72, denoting a significant influence, particularly over boreal forests, in central Africa and South America. These regions, highlighted in red in Figure 3a, represent 36% of the burnable ecoregion domain. On the other hand, SPEIc shows a similar, although slightly lower (as absolute values), sensitivity of -0.71 (SPEI is negative for hot and dry conditions) over a smaller proportion of the domain, 28% of the ecoregions. SPEIc, shown in shades of blue in Figure 3a, comprises parts of South America and Africa, as well as specific areas of Southeast Asia, some ecoregions in Australia, North America, and Siberia. The best periods and time scales for determining CC are shown in Figures 3b and 3c. The time when the concurrent climatic conditions exert the greatest influence on the overall burned area tends to coincide with the end of the fire season under consideration, as Figure 3b suggests. Indeed, the optimal month for calculating CC coincides with the end of the fire season or with the immediately preceding month (over 50% of the ecoregions), the remainder ranging between month -2 and -7 (14%). Figure 3c shows a predominant selection of short-term drought/fire weather conditions (3 months, over 31% of the ecoregions) over medium-term (6 months with 18%) and long-term

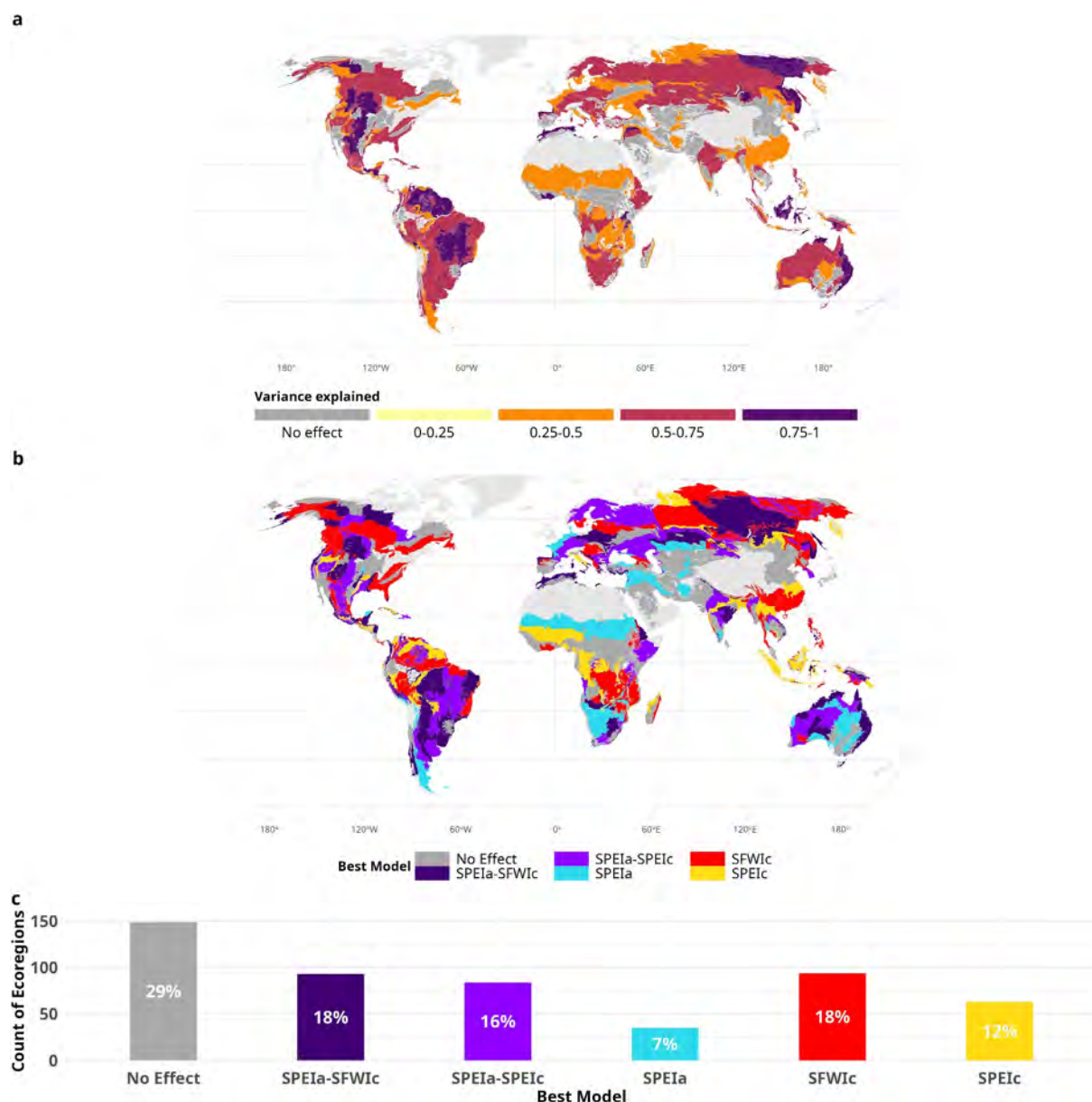


Figure 2. Burned area variability explained by climate. (a) Total BA variability explained by climate variability over the period 2001–2021. Ecoregions with non-significant models (p -value > 0.05) are represented as “No effect.” Over land, light gray denotes ecoregions where the burned area was zero in more than half of the series. (b) Selected models explaining BA variability classified into five categories of climatic drivers. The SPEIc and SFWIc models consider only concurrent (same fire season) variables. The SPEIa model considers antecedent SPEI, that is, values prior to the fire season. (c) Frequency histogram of the five models selected over the ecoregions to explain BA variability. Ecoregions with non-significant models (p -value > 0.05) are represented in dark gray.

conditions (12 months with 16%). The spatial distribution of the data exhibits no discernible pattern, often presenting adjacent ecoregions with the shortest and longest aggregation periods side by side.

3.3. Burned Area and Antecedent Weather

The sensitivity of BA to the SPEIa index (Figure 4a) shows the variation of BAI to a unit change of this (standardised) antecedent variable. According to the data, approximately 41% of the ecoregions show a significant link between BA and SPEIa. The analysis reveals that the sensitivity of BA to SPEIa is 0.52 (Table 1) denoting a significant influence in South America, North America, Sub-Saharan Africa, and Australia, and locally in Europe and Asia. Based on the observed antecedent climate effect, it appears that high rainfall and cool

Table 1
Summary Statistics of the Influence of Climate on the Burned Area Variability

Statistic	Values
Variance explained (global median)	0.60
Percentage of the domain with statistically significant influence of climate variability on burned area variability	71% (of the ecoregions) 77% (of the total surface)
Burned area sensitivity to concurrent SFWIc index (global median)	0.72
Percentage of the domain with statistically significant influence of concurrent SFWIc	36% (of the ecoregions) 36% (of the total surface)
Burned area sensitivity to concurrent SPEIc index (global median)	−0.71
Percentage of the domain with statistically significant influence of concurrent SPEIc	28% (of the ecoregions) 27% (of the total surface)
Burned area sensitivity to antecedent SPEIa index (global median)	0.52
Percentage of the domain with statistically significant influence of antecedent climate variability (SPEIa) on burned area variability	41% (of the ecoregions) 47% (of the total surface)

conditions, which can be indicative of a large amount of water in the soil, before the fire season can potentially result in higher biomass production. As a result, fuel continuity is sustained, leading to an increase in subsequent fire activity.

The periods and best time scales for determining the antecedent SPEIa are shown in Figures 4b and 4c. The optimal month for calculating the AC does not show a defined pattern (Figure 4b). Specifically, for 20% of the ecoregions, the optimal month to compute the antecedent SPEI ranges from 7 to 2 months before the fire season onset. For another 21% of the ecoregions, this optimal period extends further, from 14 to 8 months before the start of the fire season. Also, the spatial distribution of the optimal aggregation periods (3, 6, or 12 months; Figure 4c) for the antecedent climate indicators does not show a defined pattern. The best time scale, as evidenced by 3-month climatic windows, covers 15% of the burnable ecoregions selected in South America, Africa, South and Southeast Asia. The remaining 26% is evenly distributed between 6 and 12-month scales selected in Africa, North Australia, North America, and locally in Europe and Asia.

3.4. Characteristics of the Climate-Fire Links

To investigate the potential climatic drivers behind spatial variations in climate-fire associations, we examined the climatology of both the annual potential evapotranspiration and the annual precipitation averaged over the study period. Table 2 presents an assessment of the relationships between these averages and the variance explained by the climate-fire models, as well as with the CC and AC coefficients, using GAMs. The spatial variability in the strength of the climate-fire associations, as quantified by the variance explained values of the models, does not exhibit any clear patterns (as also shown in Figure 2a). This observation is further supported by the GAM results, which indicate that neither the PET nor the PREC terms are statistically significant, with p-values of 0.156 and 0.273, respectively (Table 2).

Instead, a statistically significant and distinctly non-linear (curvilinear) relationship emerges between PET and the Concurrent Climate coefficients, as detailed in Table 2 and shown in Figures 5a and 5b. As illustrated in Figure 5a, these coefficients maintain similar magnitudes in regions with a mean annual PET below roughly 400 mm/y. Instead, in areas where the mean annual PET surpasses this value, there is a marked decrease in these coefficients. Furthermore, the relationship with precipitation tends toward linearity and, although is weaker than that with PET, it remains statistically significant (Table 2). As Figure 5b delineates, ecoregions with higher climatological precipitation amounts feature larger Concurrent Climate coefficients. Shifting focus to the Antecedent Climate coefficients (Figures 5c and 5d), the influence is marginally more pronounced (see Table 2). These coefficients display a considerable surge in regions where PET exceeds 400 mm/y (Figure 5c). Also, there is a mostly linear decrease in these weights as precipitation increases, plateauing around 2000 mm/y. Beyond this threshold, a discernible pattern remains elusive (Figure 5d).

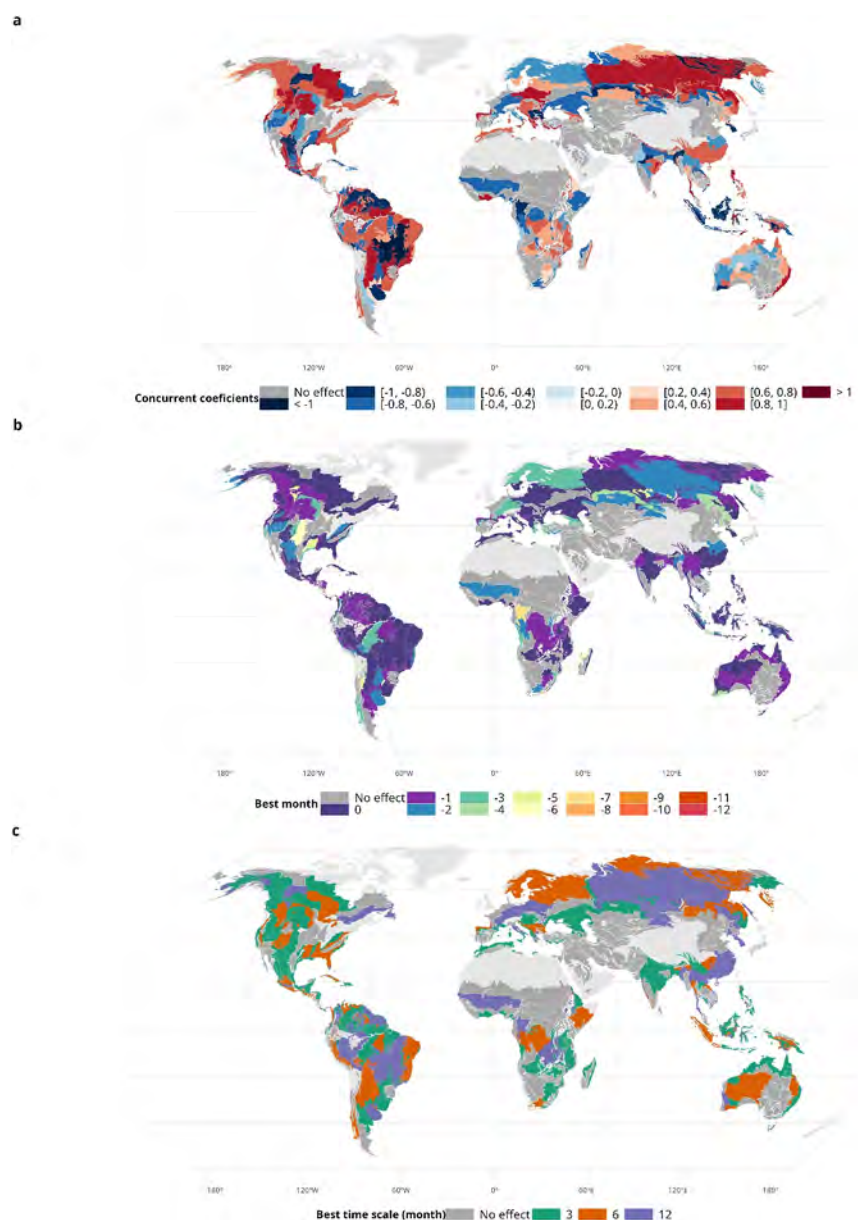


Figure 3. Links of burned area to concurrent climatic variables. (a) Sensitivity of burned area to concurrent climatic variables (i.e., SFWIc or SPEIc indices). Ecoregions with non-significant models (p -value > 0.05) are represented as “No effect.” Over land, light gray denotes ecoregions where the burned area was zero in more than half of the series. (b) Refers to the number of months prior to the end of the fire season that were used to calculate the SFWIc or SPEIc indices. (c) Best time scale (3, 6 or 12 months) selected by the statistical analysis for calculating SFWIc or SPEIc indices.

4. Discussion and Conclusion

In this study, we explored whether and to what extent climate variability can account for the year-to-year fluctuations in burned area at the global scale, considering an ecoregion's resolution. Our analysis indicates that climate variability is a significant determinant of BA, influencing 71% of ecoregions and covering 77% of the burnable surface. Notably, in areas with statistically significant fire-climate connections, climate variability accounts for about 60% of BA fluctuations, aligning with prior regional studies (see e.g., Balshi et al., 2009; Bedia et al., 2014; Canadell et al., 2021; Girardin & Wotton, 2009; Littell et al., 2009; Turco et al., 2017, 2023; Urbietta et al., 2015; Vadrevu et al., 2019; Zubkova et al., 2019). Our results, which extend these regional studies to global scales, can be used to identify regions with a strong relationship between climate and fire that may undergo

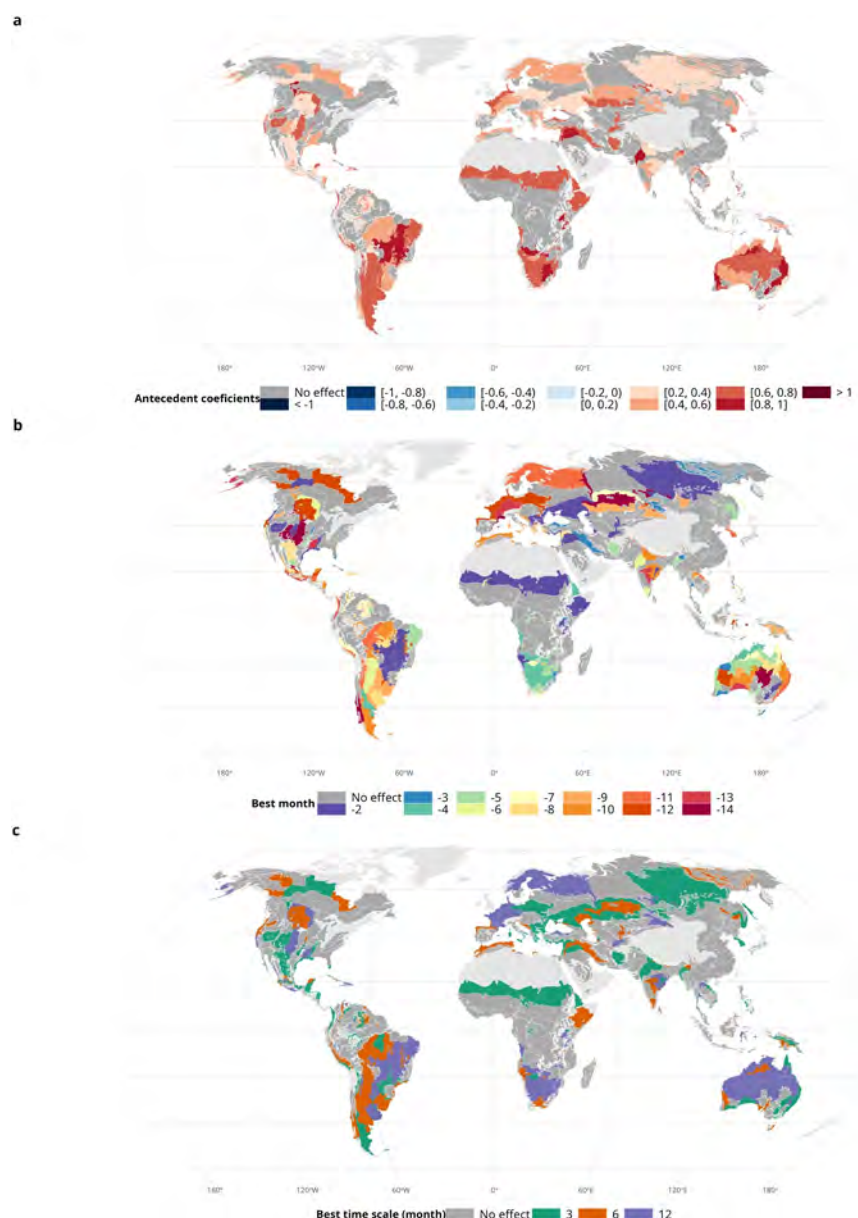


Figure 4. Burned area sensitivity to antecedent climate variable. (a) Positive SPEI indicates wetter conditions and positive SPEI coefficients imply larger burned area values. Ecoregions with non-significant models (p -value > 0.05) are represented as “No effect.” Over land, light gray denotes ecoregions where the burned area was zero in more than half of the series. (b) Months before the start of the fire season that are selected by statistical analysis to calculate the SPEI index. (c) Best time scale (3, 6 or 12 months) selected for calculating the SPEI index.

significant changes in the forthcoming decades (e.g., Pechony & Shindell, 2010; Senande-Rivera et al., 2022). Also, while global assessments of temporal climate-fires links are scarce, our work contributes to this limited body of research. The recent review by Jones et al. (2022) provided a comprehensive overview of fire trends and drivers under climate change, focusing on the temporal variability of climate and fires, yet restricted its analysis to the Spearman correlation between BA and the Fire Weather Index (FWI).

Similarly, an early global study by Bedia et al. (2015) examined the temporal association between BA and concurrent FWI. Our research extends these efforts by incorporating a wider array of climate factors and constructing more complex fire-climate models. Specifically, we build on the efforts of Turco, Jerez, et al. (2018) and Abatzoglou et al. (2018), the latter of whom documented that climate variability accounted for about a third of the

Table 2

Summary Statistics (Adjusted R^2 , Deviance Explained, and p-Value) GAM Relating the Climate-Fires Model Characteristics and Potential Evapotranspiration and Precipitation Climatologies

Dependent variable	Independent variable	GAM metrics
Variance explained	PET	R-sq.(adj) = 0.022
		Deviance Explained = 3.700%
	PREC	p-value (smooth) = 0.156
		R-sq.(adj) = 0.001
		Deviance Explained = 0.328%
		p-value (smooth) = 0.273
Concurrent Climate coefficients	PET	R-sq.(adj) = 0.107
		Deviance Explained = 11.5%
		p-value (smooth) = 3.25e−07
	PREC	R-sq.(adj) = 0.0631
		Deviance Explained = 6.86%
		p-value (smooth) = 4.9e−05
Antecedent Climate coefficients	PET	R-sq.(adj) = 0.165
		Deviance Explained = 18.3%
		p-value (smooth) = 9.03e−07
	PREC	R-sq.(adj) = 0.168
		Deviance Explained = 18.9%
		p-value (smooth) = 6.5e−07

interannual BA variability. Our findings advance this by demonstrating that climate variability is responsible for a significantly larger portion of BA fluctuations —60% on average—attributable to both methodological enhancements and data updates. While Abatzoglou et al. (2018) relied on the Global Fire Emissions Database (GFED4s) for the period 1997–2016, acknowledging temporal data issues due to changes in satellite data sources, we incorporated BA data less affected by temporal inconsistencies and updated up to a more recent period (Giglio et al., 2018). Also, we employed the latest climatological data sets (ERA5 vs. ERA-Interim reanalysis, and the MSWEP version 2.8 vs. the previous version described in Beck et al., 2017) that offer considerable improvements and probably have been instrumental in revealing a stronger and more coherent relationship between climate variability and BA compared to previous findings. Our methodology also departs from Abatzoglou et al. (2018). They limited their consideration to 12-month accumulated precipitation over two specific antecedent periods. In contrast, our study tested several climate windows to compute the antecedent climate conditions and employed a False Discovery Rate test to ensure statistical integrity amidst multiple comparisons. Furthermore, our study integrates the refined ecoregion delineations from Dinerstein et al. (2017), replacing the Olson et al. (2001) map, to better capture the recent biogeographic changes. In sum, our methodological advancements have probably provided a more detailed and accurate assessment of the complex interplay between climate variability and BA.

In our analysis, we investigated the strength of climate-fire relationships across different climatic regions. Our findings indicate no significant association between the strength of these links, measured by the variance explained by the climate-fires models, and regional climatology, suggesting that climate exerts a consistent influence on fire temporal variability in both arid and humid zones. We also find that, in about 23% of the domain, climate-fire links were not statistically significant, with no clear patterns emerging. These regions might be subject to more subtle influences, such as anthropogenic factors, that overshadow the climatic signal. For example, Chuvieco et al. (2021) conducted a spatial analysis of the long-term mean of the coefficient of variation of burned area and identified the human imprint on the spatial pattern of burned area variability, particularly in areas of tropical Africa and Central Asia with low to medium fire variability. Our results align with these observations, indicating areas where the temporal climate influence on fires is absent or reduced. This weak or null climate–fire link may be also related to data quality concerns, particularly in data-deficient regions like Africa. Among the climate variables analyzed, precipitation data, in particular, carry inherent uncertainties (Sun et al., 2018). We selected the MSWEP data set for its superior performance in comparative studies (Beck, Pan,

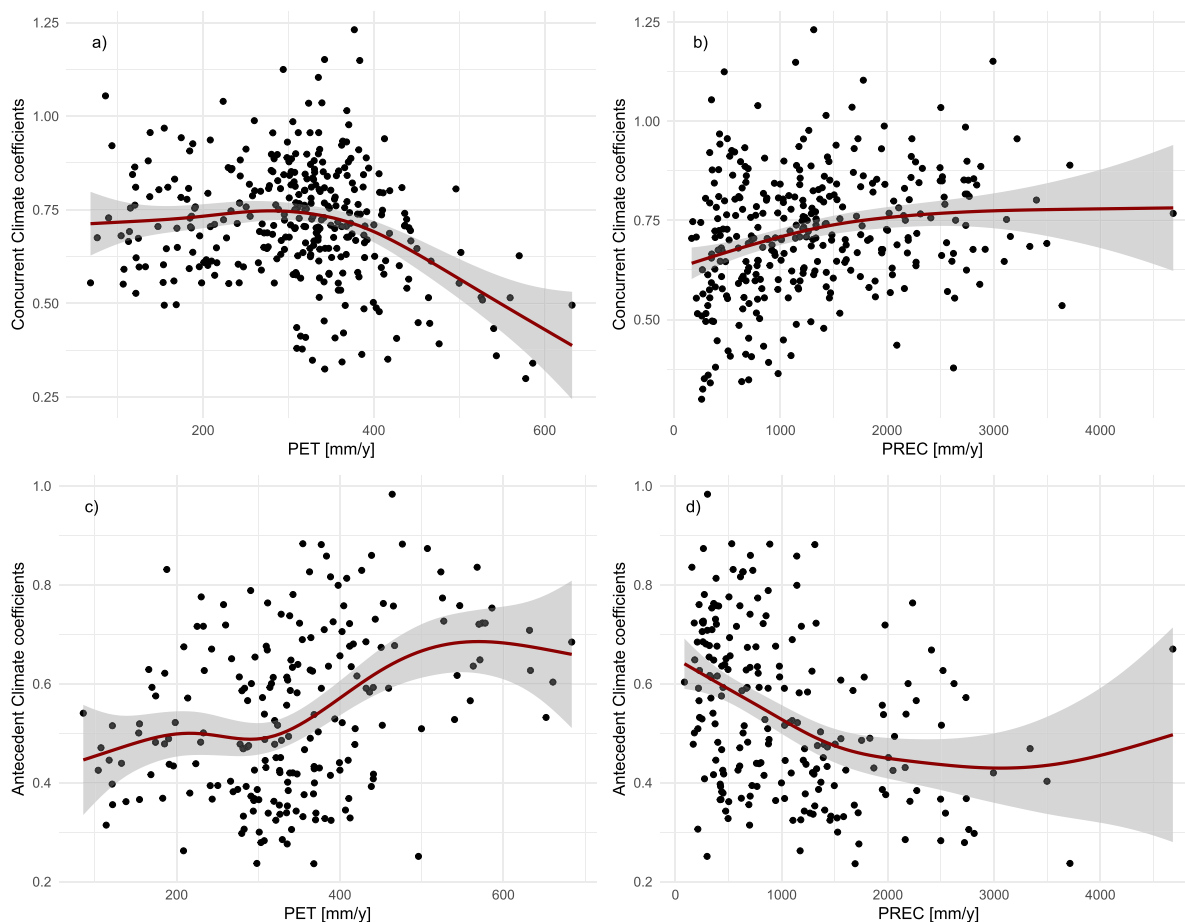


Figure 5. Scatterplots depicting the relationships between Concurrent and Antecedent Climate Coefficients with (a, c) Potential Evapotranspiration (PET) and (b, d) Precipitation (PREC) climatology. The red curve represents the non-linear fit estimated using a Generalized Additive Model (GAM), with the shaded area indicating the 95% confidence interval.

et al., 2019; Beck et al., 2017; Turco et al., 2020; Xu et al., 2019). Also, in estimating burned area, we recognize that remote sensing techniques have limitations, such as the under-detection of understory and agricultural fires, and the potential for false positives from smoke, cloud shadows, or deforestation (Campagnolo et al., 2021; Mouillot et al., 2014; Turco, Herrera, et al., 2019). To ensure robustness, we compared two BA products and accounted for agricultural fires through different processing methods, obtaining generally consistent results across analyses. Despite these measures, the inherent uncertainties in climate and fire data remain a challenge. A notable limitation is the relatively short duration of global BA data sets, which have only been reliably available since the early 2000s (Chuvieco et al., 2019). This limitation is significant for interpreting temporal patterns in regions with low-frequency fire activity and for deriving temporal relationships from a limited data sample. As satellite-based BA estimates become increasingly prevalent in fire research, the need for long-term data to enhance our understanding of these relationships becomes ever more critical.

Our study deepens the comprehension of how same-season (CC) and antecedent-season climate (AC) factors affect burned area (BA) by employing a regression model that captures their combined influence. We observed that CC generally exerts a stronger influence on BA than AC, with the Fire Weather Index (FWI) being a particularly effective concurrent climate metric, more so than the Standardized Precipitation Evapotranspiration Index (SPEI). CC is notably dominant in shaping BA in wetter climates, whereas AC has a pronounced impact in arid regions. These findings align with and extend the work of Abatzoglou et al. (2018), Jones et al. (2022), and Qu et al. (2023), which underscored the critical role of fire weather as a “top-down” driver of BA variability, especially in high-latitude forests. Our research corroborates this and further delineates how the FWI and the SPEI climate indices differentially influence BA. The insights gained from this study may have implications for

predicting future fire activity amidst climate change. While projections indicate an increased meteorological risk of fires (IPCC, 2021), this does not necessarily translate to a corresponding rise in BA due to the potential counteracting effects of other drivers (Pausas & Keeley, 2021). Climate-driven variations in precipitation, temperature, vegetation, and human activities all contribute to fire responses (Jones et al., 2022). In areas where climate trends toward warmer and drier conditions, the direct effect on fuel moisture suggests larger BA values (Ellis et al., 2022; Resco de Dios et al., 2022; Turco et al., 2014). However, in arid regions, BA is often linked to prior wet and cool periods, particularly in grass-dominated ecosystems where antecedent climate has a significant impact on biomass (Resco de Dios et al., 2022). This implies that increasingly hot and dry conditions could paradoxically reduce BA by constraining vegetation growth. Given that our findings indicate a dominance of CC over AC in many ecoregions, a stationary climate-fire link would suggest that hotter and drier future conditions could increase BA in those ecoregions. Yet, direct extrapolation of BA from present climate-fire models may lead to an overestimation. It is perhaps more prudent to consider potential changes in the climate-fire relationship due to shifts in productivity and fuel structure driven by climate change.

This assessment of global temporal climate-fire links at ecoregion resolution can serve as a baseline for future analyses. Ultimately, our results can offer a clear indication of where to focus mitigation efforts and further research to better understand and manage fire landscapes under changing climate conditions. Future directions could include investigating the frequency and intensity of large fires, improving climate-fire data sets, using more complex empirical models, and exploring other climatic variables such as wind speed, soil moisture, and climate extremes. As global fire and climate data sets improve in duration and quality, climate-fire models are expected to become more accurate. Notwithstanding current limitations, our results indicate that the predominance of climate in determining BA fluctuations presents a challenge, as it limits the efficacy of management strategies against the backdrop of uncontrollable climate variability. This underscores the urgent need for adaptive management practices that can mitigate the risks posed by changing fire regimes.

Data Availability Statement

The specific data used in this study are as follows: FireCCI51 data as reported by Lizundia-Loiola et al. (2020) and available at (Chuvieco et al., 2018). The MCD64CMQ data set from Giglio et al. (2018). The FWI data set detailed by Vitolo et al. (2020) and available at Copernicus Climate Change Service, Climate Data Store, (2019). The SPEI, developed by Vicente-Serrano et al. (2022), utilizes ERA5 data as detailed in Hersbach et al. (2023). PET was estimated based on ERA5 data available by Hersbach et al. (2020). For PREC we used the MSWEP data set as documented by Beck, Wood, et al. (2019). All codes needed to reproduce the results of this study are available in Gincheva and Turco (2023).

Acknowledgments

A.G. thanks the Ministerio de Ciencia, Innovación y Universidades of Spain for PhD contract FPU19/06536 and extends his thanks to the Instituto Dom Luiz for its close collaboration during her stay in Lisbon. A.G., M.A.T.-V., S.J., and M.T. acknowledges the support of the ONFIRE project, Grant PID2021-123193OB-I00, funded by MCIN/AEI/10.13039/501100011033 and by "ERDF A way of making Europe." M.T. acknowledges funding by the Spanish Ministry of Science, Innovation, and Universities through the Ramón y Cajal Grant Reference RYC2019-027115-I. S.J. acknowledges funding by the Spanish Ministry of Science, Innovation, and Universities through the Ramón y Cajal Grant Reference RYC2020-029993-I.

References

- Abatzoglou, J. T., & Williams, A. P. (2016). Impact of anthropogenic climate change on wildfire across western US forests. *Proceedings of the National Academy of Sciences of the United States of America*, 113(42), 11770–11775. <https://doi.org/10.1073/pnas.1607171113>
- Abatzoglou, J. T., Williams, A. P., Boschetti, L., Zubkova, M., & Kolden, C. A. (2018). Global patterns of interannual climate–fire relationships. *Global Change Biology*, 24(11), 5164–5175. <https://doi.org/10.1111/gcb.14405>
- Balshi, M. S., McGuire, A. D., Duffy, P., Flannigan, M., Walsh, J., & Melillo, J. (2009). Assessing the response of area burned to changing climate in western boreal North America using a Multivariate Adaptive Regression Splines (MARS) approach. *Global Change Biology*, 15(3), 578–600. <https://doi.org/10.1111/j.1365-2486.2008.01679.x>
- Beck, H. E., Pan, M., Roy, T., Weedon, G. P., Pappenberger, F., Van Dijk, A. I., et al. (2019). Daily evaluation of 26 precipitation datasets using Stage-IV gauge-radar data for the CONUS. *Hydrology and Earth System Sciences*, 23(1), 207–224. <https://doi.org/10.5194/hess-23-207-2019>
- Beck, H. E., van Dijk, A. I. J. M., Levizzani, V., Schellekens, J., Miralles, D. G., Martens, B., & de Roo, A. (2017). MSWEP: 3-hourly 0.25 global gridded precipitation (1979–2015) by merging gauge, satellite, and reanalysis data. *Hydrology and Earth System Sciences*, 21(1), 589–615. <https://doi.org/10.5194/hess-21-589-2017>
- Beck, H. E., Wood, E. F., Pan, M., Fisher, C. K., Miralles, D. G., van Dijk, A. I. J. M., et al. (2019). MSWEP V2 global 3-hourly 0.1° precipitation: Methodology and quantitative assessment [Dataset]. *Bulletin of the American Meteorological Society*, 100(3), 473–500. <https://doi.org/10.1175/BAMS-D-17-0138.1>
- Bedia, J., Herrera, S., & Gutiérrez, J. M. (2014). Assessing the predictability of fire occurrence and area burned across phytoclimatic regions in Spain. *Natural Hazards and Earth System Sciences*, 14(1), 53–66. <https://doi.org/10.5194/nhess-14-53-2014>
- Bedia, J., Herrera, S., Gutiérrez, J. M., Benali, A., Brands, S., Mota, B., & Moreno, J. M. (2015). Global patterns in the sensitivity of burned area to fire weather: Implications for climate change. *Agricultural and Forest Meteorology*, 214, 369–379. <https://doi.org/10.1016/j.agrformet.2015.09.002>
- Bowman, D. M. (2018). Wildfire science is at a loss for comprehensive data. *Nature*, 560(7716), 7–8. <https://doi.org/10.1038/d41586-018-05840-4>
- Bowman, D. M., Kolden, C. A., Abatzoglou, J. T., Johnston, F. H., vander Werf, G. R., & Flannigan, M. (2020). Vegetation fires in the anthropocene. *Nature Reviews Earth and Environment*, 1(10), 500–515. <https://doi.org/10.1038/s43017-020-0085-3>

- Breusch, T. S., & Pagan, A. R. (1979). A simple test for heteroscedasticity and random coefficient variation. *Econometrica*, 47(5), 1287–1294. <https://doi.org/10.2307/1911963>
- Campagnolo, M. L., Libonati, R., Rodrigues, J. A., & Pereira, J. M. C. (2021). A comprehensive characterization of MODIS daily burned area mapping accuracy across fire sizes in tropical savannas. *Remote Sensing of Environment*, 252, 112115. <https://doi.org/10.1016/j.rse.2020.112115>
- Canadell, J. G., Meyer, C. P., Cook, G. D., Dowdy, A., Briggs, P. R., Knauer, J., et al. (2021). Multi-decadal increase of forest burned area in Australia is linked to climate change. *Nature Communications*, 12(1), 1–11. <https://doi.org/10.1038/s41467-021-27225-4>
- Chen, Y., Morton, D. C., Andela, N., Giglio, L., & Randerson, J. T. (2016). How much global burned area can be forecast on seasonal time scales using sea surface temperatures? *Environmental Research Letters*, 11(4), 045001. <https://doi.org/10.1088/1748-9326/11/4/045001>
- Chuvieco, E., Mouillot, F., Van der Werf, G. R., San Miguel, J., Tanase, M., Koutsias, N., et al. (2019). Historical background and current developments for mapping burned area from satellite Earth observation. *Remote Sensing of Environment*, 225, 45–64. <https://doi.org/10.1016/j.rse.2019.02.013>
- Chuvieco, E., Pettinari, M. L., Koutsias, N., Forkel, M., Hantson, S., & Turco, M. (2021). Human and climate drivers of global biomass burning variability. *Science of the Total Environment*, 779, 146361. <https://doi.org/10.1016/j.scitotenv.2021.146361>
- Chuvieco, E., Pettinari, M. L., Lizundia-Loiola, J., Storm, T., & Padilla Parellada, M. (2018). ESA fire climate change initiative (Fire_cci): MODIS Fire_cci burned area pixel product, version 5.1 [Dataset]. *Centre for Environmental Data Analysis*. <https://doi.org/10.5285/58f00d8814064b79a0c49662ad3af537>
- Copernicus Climate Change Service, Climate Data Store. (2019). Fire danger indices historical data from the copernicus emergency management service [Dataset]. *Copernicus Climate Change Service (C3S) Climate Data Store (CDS)*. <https://doi.org/10.24381/cds.0e89c522>
- Coughlan, M. R., Ellison, A., & Cavanaugh, A. H. (2019). *Social vulnerability and wildfire in the wildland-urban interface: Literature synthesis [Working Paper]*. Ecosystem Workforce Program, Institute for a Sustainable Environment, University of Oregon. Retrieved from <https://scholarsbank.uoregon.edu/xmlui/handle/1794/25359>
- Dinerstein, E., Olson, D., Joshi, A., Vynne, C., Burgess, N. D., Wikramanayake, E., et al. (2017). An ecoregion-based approach to protecting half the terrestrial realm. *BioScience*, 67(6), 534–545. <https://doi.org/10.1093/biosci/bix014>
- Durbin, J., & Watson, G. S. (1950). Testing for serial correlation in least squares regression. *Biometrika*, 37(3–4), 409–428. <https://doi.org/10.1093/biomet/37.3-4.409>
- Ellis, T. M., Bowman, D. M. J. S., Jain, P., Flannigan, M. D., & Williamson, G. J. (2022). Global increase in wildfire risk due to climate-driven declines in fuel moisture. *Global Change Biology*, 28(4), 1544–1559. <https://doi.org/10.1111/gcb.16006>
- Giglio, L., Boschetti, L., Roy, D. P., Humber, M. L., & Justice, C. O. (2018). The Collection 6 MODIS burned area mapping algorithm and product [Dataset]. *Remote Sensing of Environment*, 217, 72–85. <https://doi.org/10.1016/j.rse.2018.08.005>
- Gincheva, A., & Turco, M. (2023). Climate-Fire model (Version v1) [Software]. *Zenodo*. <https://doi.org/10.5281/zenodo.10410211>
- Girardin, M. P., & Wotton, B. M. (2009). Summer moisture and wildfire risks across Canada. *Journal of Applied Meteorology and Climatology*, 48(3), 517–533. <https://doi.org/10.1175/2008jamc1996.1>
- Grillakis, M., Voulgarakis, A., Rovithakis, A., Seiradakis, K. D., Koutroulis, A., Field, R. D., et al. (2022). Climate drivers of global wildfire burned area. *Environmental Research Letters*, 17(4), 045021. <https://doi.org/10.1088/1748-9326/ac5fa1>
- Hersbach, H., Bell, B., Berrisford, P., Biavati, G., Horányi, A., Muñoz Sabater, J., et al. (2023). ERA5 hourly data on single levels from 1940 to present [Dataset]. *Copernicus Climate Change Service (C3S) Climate Data Store (CDS)*. <https://doi.org/10.24381/cds.adbb2d47>
- Hersbach, H., Bell, B., Berrisford, P., Hirahara, S., Horányi, A., Muñoz-Sabater, J., et al. (2020). The ERA5 global reanalysis [Dataset]. *Quarterly Journal of the Royal Meteorological Society*, 146(730), 1999–2049. <https://doi.org/10.1002/qj.3803>
- IPCC. (2021). In V. Masson-Delmotte, P. Zhai, A. Pirani, S. L. Connors, C. Péan, et al. (Eds.), *Climate Change 2021: The Physical Science Basis. Contribution of Working Group I to the Sixth Assessment Report of the Intergovernmental Panel on Climate Change* (p. 2391). Cambridge University Press. <https://doi.org/10.1017/9781009157896>
- Jones, M. W., Abatzoglou, J. T., Veraverbeke, S., Andela, N., Lasslop, G., Forkel, M., et al. (2022). Global and regional trends and drivers of fire under climate change. *Reviews of Geophysics*, 60(3), e2020RG000726. <https://doi.org/10.1029/2020rg000726>
- Kato, T., Kobayashi, A., Oishi, W., Kadoya, S. S., Okabe, S., Ohta, N., et al. (2019). Sign-constrained linear regression for prediction of microbe concentration based on water quality datasets. *Journal of Water and Health*, 17(3), 404–415. <https://doi.org/10.2166/wh.2019.001>
- Krawchuk, M. A., & Moritz, M. A. (2011). Constraints on global fire activity vary across a resource gradient. *Ecology*, 92(1), 121–132. <https://doi.org/10.1890/09-1843.1>
- Le Page, Y., Pereira, J. M. C., Trigo, R., da Camara, C., Oom, D., & Mota, B. (2008). Global fire activity patterns (1996–2006) and climatic influence: An analysis using the world fire atlas. *Atmospheric Chemistry and Physics*, 8(7), 1911–1924. <https://doi.org/10.5194/acp-8-1911-2008>
- Littell, J. S., McKenzie, D., Peterson, D. L., & Westerling, A. L. (2009). Climate and wildfire area burned in western U.S. ecoprovinces, 1916–2003. *Ecological Applications*, 19(4), 1003–1021. <https://doi.org/10.1890/07-1183.1>
- Lizundia-Loiola, J., Otón, G., Ramo, R., & Chuvieco, E. (2020). A spatio-temporal active-fire clustering approach for global burned area mapping at 250 m from MODIS data. *Remote Sensing of Environment*, 236, 111493. <https://doi.org/10.1016/j.rse.2019.111493>
- Marcos, R., Turco, M., Bedia, J., Llasat, M. C., & Provenzale, A. (2015). Seasonal predictability of summer fires in a mediterranean environment. *International Journal of Wildland Fire*, 24(8), 1076. <https://doi.org/10.1071/wf15079>
- Massey, F. J., Jr. (1951). The Kolmogorov-Smirnov test for goodness of fit. *Journal of the American Statistical Association*, 46(253), 68–78. <https://doi.org/10.2307/2280095>
- Mouillot, F., Schultz, M. G., Yue, C., Cadule, P., Tansey, K., Ciais, P., & Chuvieco, E. (2014). Ten years of global burned area products from spaceborne remote sensing—A review: Analysis of user needs and recommendations for future developments. *International Journal of Applied Earth Observation and Geoinformation*, 26, 64–79. <https://doi.org/10.1016/j.jag.2013.05.014>
- Olson, D. M., Dinerstein, E., Wikramanayake, E. D., Burgess, N. D., Powell, G. V. N., Underwood, E. C., et al. (2001). Terrestrial ecoregions of the world: A new map of life on Earth: A new global map of terrestrial ecoregions provides an innovative tool for conserving biodiversity. *BioScience*, 51(11), 933–938. [https://doi.org/10.1641/0006-3568\(2001\)051\[0933:TEOTWA\]2.0.CO;2](https://doi.org/10.1641/0006-3568(2001)051[0933:TEOTWA]2.0.CO;2)
- Parks, S. A., & Abatzoglou, J. T. (2020). Warmer and drier fire seasons contribute to increases in area burned at high severity in western US forests from 1985 to 2017. *Geophysical Research Letters*, 47(22), e2020GL089858. <https://doi.org/10.1029/2020GL089858>
- Pausas, J. G. (2022). Pyrogeography across the western palaearctic: A diversity of fire regimes. *Global Ecology and Biogeography*, 31(10), 1923–1932. <https://doi.org/10.1111/geb.13569>
- Pausas, J. G., & Keeley, J. E. (2021). Wildfires and global change. *Frontiers in Ecology and the Environment*, 19(7), 387–395. <https://doi.org/10.1002/fee.2359>

- Pechony, O., & Shindell, D. T. (2010). Driving forces of global wildfires over the past millennium and the forthcoming century. *Proceedings of the National Academy of Sciences of the United States of America*, 107(45), 19167–19170. <https://doi.org/10.1073/pnas.1003669107>
- Qu, Y., Miralles, D. G., Veraverbeke, S., Vereecken, H., & Montzka, C. (2023). Wildfire precursors show complementary predictability in different timescales. *Nature Communications*, 14(1), 6829. <https://doi.org/10.1038/s41467-023-42597-5>
- Ramo, R., Roteta, E., Bistinas, I., van Wees, D., Bastarrika, A., Chuvieco, E., & van der Werf, G. R. (2021). African burned area and fire carbon emissions are strongly impacted by small fires undetected by coarse resolution satellite data. *Proceedings of the National Academy of Sciences of the United States of America*, 118(9), e2011160118. <https://doi.org/10.1073/pnas.2011160118>
- Resco de Dios, V., Cunill Camprubí, À., Pérez-Zanón, N., Peña, J. C., Martínez del Castillo, E., Rodrigues, M., et al. (2022). Convergence in critical fuel moisture and fire weather thresholds associated with fire activity in the pyroregions of Mediterranean Europe. *Science of the Total Environment*, 806, 151462. <https://doi.org/10.1016/j.scitotenv.2021.151462>
- Senande-Rivera, M., Insua-Costa, D., & Miguez-Macho, G. (2022). Spatial and temporal expansion of global wildland fire activity in response to climate change. *Nature Communications*, 13(1), 1208. <https://doi.org/10.1038/s41467-022-28835-2>
- Shen, H., Tao, S., Chen, Y., Odman, M. T., Zou, Y., Huang, Y., et al. (2019). Global fire forecasts using both large-scale climate indices and local meteorological parameters. *Global Biogeochemical Cycles*, 33(8), 1129–1145. <https://doi.org/10.1029/2019gb006180>
- Silvapulle, M. J., & Sen, P. K. (2005). *Constrained statistical inference: Inequality, order and shape restrictions*. John Wiley & Sons.
- Stone, M. (1977). An asymptotic equivalence of choice of model by cross-validation and Akaike's criterion. *Journal of the Royal Statistical Society: Series B*, 39(1), 44–47. <https://doi.org/10.1111/j.2517-6161.1977.tb01603.x>
- Sun, Q., Miao, C., Duan, Q., Ashouri, H., Sorooshian, S., & Hsu, K.-L. (2018). A review of global precipitation data sets: Data sources, estimation, and intercomparisons. *Reviews of Geophysics*, 56(1), 79–107. <https://doi.org/10.1002/2017rg000574>
- Tong, H. (1990). *Nonlinear time series: A dynamical system approach*. Oxford University Press.
- Turco, M., Abatzoglou, J. T., Herrera, S., Zhuang, Y., Jerez, S., Lucas, D. D., et al. (2023). Anthropogenic climate change impacts exacerbate summer forest fires in California. *Proceedings of the National Academy of Sciences of the United States of America*, 120(25), e2213815120. <https://doi.org/10.1073/pnas.2213815120>
- Turco, M., Herrera, S., Tourigny, E., Chuvieco, E., & Provenzale, A. (2019). A comparison of remotely-sensed and inventory datasets for burned area in Mediterranean Europe. *International Journal of Applied Earth Observation and Geoinformation*, 82, 101887. <https://doi.org/10.1016/j.jag.2019.05.020>
- Turco, M., Jerez, S., Augusto, S., Tarín-Carrasco, P., Ratola, N., Jiménez-Guerrero, P., & Trigo, R. M. (2019). Climate drivers of the 2017 devastating fires in Portugal. *Scientific Reports*, 9(1), 1–8. <https://doi.org/10.1038/s41598-019-50281-2>
- Turco, M., Jerez, S., Doblas-Reyes, F. J., AghaKouchak, A., Llasat, M. C., & Provenzale, A. (2018). Skillful forecasting of global fire activity using seasonal climate predictions. *Nature Communications*, 9(1), 1–9. <https://doi.org/10.1038/s41467-018-05250-0>
- Turco, M., Jerez, S., Donat, M. G., Toreti, A., Vicente-Serrano, S. M., & Doblas-Reyes, F. J. (2020). A global probabilistic dataset for monitoring meteorological droughts. *Bulletin of the American Meteorological Society*, 101(10), E1628–E1644. <https://doi.org/10.1175/bams-d-19-0192.1>
- Turco, M., Llasat, M.-C., von Hardenberg, J., & Provenzale, A. (2014). Climate change impacts on wildfires in a Mediterranean environment. *Climatic Change*, 125(3), 369–380. <https://doi.org/10.1007/s10584-014-1183-3>
- Turco, M., Rosa-Cánovas, J. J., Bedia, J., Jerez, S., Montávez, J. P., Llasat, M. C., & Provenzale, A. (2018). Exacerbated fires in Mediterranean Europe due to anthropogenic warming projected with non-stationary climate-fire models. *Nature Communications*, 9(1), 1–9. <https://doi.org/10.1038/s41467-018-06358-z>
- Turco, M., von Hardenberg, J., AghaKouchak, A., Llasat, M. C., Provenzale, A., & Trigo, R. M. (2017). On the key role of droughts in the dynamics of summer fires in Mediterranean Europe. *Scientific Reports*, 7(1), 1–10. <https://doi.org/10.1038/s41598-017-00116-9>
- Urbieto, I. R., Zavala, G., Bedia, J., Gutiérrez, J. M., San Miguel-Ayán, J., Camia, A., et al. (2015). Fire activity as a function of fire– weather seasonal severity and antecedent climate across spatial scales in southern Europe and Pacific western USA. *Environmental Research Letters*, 10(11), 114013. <https://doi.org/10.1088/1748-9326/10/11/114013>
- Vadrevu, K. P., Lasko, K., Giglio, L., Schroeder, W., Biswas, S., & Justice, C. (2019). Trends in vegetation fires in South and Southeast Asian Countries. *Scientific Reports*, 9(1), 7422. <https://doi.org/10.1038/s41598-019-43940-x>
- Ventura, V., Paciorek, C. J., & Risbey, J. S. (2004). Controlling the proportion of falsely rejected hypotheses when conducting multiple tests with climatological data. *Journal of Climate*, 17(22), 4343–4356. <https://doi.org/10.1175/3199.1>
- Vicente-Serrano, S. M., Beguería, S., & López-Moreno, J. I. (2010). A multiscalar drought index sensitive to global warming: The standardized precipitation evapotranspiration index. *Journal of Climate*, 23(7), 1696–1718. <https://doi.org/10.1175/2009jcli2909.1>
- Vicente-Serrano, S. M., Beguería, S., Lorenzo-Lacruz, J., Camarero, J. J., López-Moreno, J. I., Azorin-Molina, C., et al. (2012). Performance of drought indices for ecological, agricultural, and hydrological applications. *Earth Interactions*, 16(10), 1–27. <https://doi.org/10.1175/2012ei000434.1>
- Vicente-Serrano, S. M., Domínguez-Castro, F., Reig, F., Tomas-Burguera, M., Peña-Angulo, D., Latorre, B., et al. (2022). A global drought monitoring system and dataset based on ERA5 reanalysis: A focus on crop-growing regions. *Geoscience Data Journal*, 10(4), 505–518. <https://doi.org/10.1002/gdj3.178>
- Vitolo, C., Di Giuseppe, F., Barnard, C., Coughlan, R., San-Miguel-Ayán, J., Libertá, G., & Krzeminski, B. (2020). ERA5-based global meteorological wildfire danger maps. *Scientific Data*, 7(1), 216. <https://doi.org/10.1038/s41597-020-0554-z>
- Xu, Z., Wu, Z., He, H., Wu, X., Zhou, J., Zhang, Y., & Guo, X. (2019). Evaluating the accuracy of MSWEP V2.1 and its performance for drought monitoring over mainland China. *Atmospheric Research*, 226, 17–31. <https://doi.org/10.1016/j.atmosres.2019.04.008>
- Xystrakis, F., Kallimanis, A. S., Dimopoulos, P., Halley, J. M., & Koutsias, N. (2014). Precipitation dominates fire occurrence in Greece (1900–2010): Its dual role in fuel build-up and dryness. *Natural Hazards and Earth System Sciences*, 14(1), 21–32. <https://doi.org/10.5194/nhess-14-21-2014>
- Zubkova, M., Boschetti, L., Abatzoglou, J. T., & Giglio, L. (2019). Changes in fire activity in Africa from 2002 to 2016 and their potential drivers. *Geophysical Research Letters*, 46(13), 7643–7653. <https://doi.org/10.1029/2019GL083469>
- Zuur, A. F., Ieno, E. N., & Elphick, C. S. (2010). A protocol for data exploration to avoid common statistical problems. *Methods in Ecology and Evolution*, 1(1), 3–14. <https://doi.org/10.1111/j.2041-210X.2009.00001.x>